



Published in final edited form as:

*Biochemistry*. 2015 May 26; 54(20): 3173–3182. doi:10.1021/acs.biochem.5b00303.

## Cancer-Associated Mutations in Breast Tumor Kinase/PTK6 Differentially Affect Enzyme Activity and Substrate Recognition

Tiffany Tsui and W. Todd Miller\*

Department of Physiology and Biophysics, School of Medicine, Stony Brook University, Stony Brook, New York 11794, United States

### Abstract

Brk (breast tumor kinase, also known as PTK6) is a nonreceptor tyrosine kinase that is aberrantly expressed in several cancers and promotes cell proliferation and transformation. Genome sequencing studies have revealed a number of cancer-associated somatic mutations in the Brk gene; however, their effect on Brk activity has not been examined. We analyzed a panel of cancer-associated mutations and determined that several of the mutations activate Brk, while two eliminated enzymatic activity. Three of the mutations (L16F, R131L, and P450L) are located in important regulatory domains of Brk (the SH3, SH2 domains, and C-terminal tail, respectively). Biochemical data suggest that they activate Brk by disrupting intramolecular interactions that normally maintain Brk in an autoinhibited conformation. We also observed differential effects on recognition and phosphorylation of substrates, suggesting that the mutations can influence downstream Brk signaling by multiple mechanisms.

### Graphical abstract



Brk (Breast tumor kinase, also known as PTK6) is a nonreceptor tyrosine kinase that is a member of the family of kinases that includes Frk, Srms, and Sik.<sup>1</sup> Brk has 46% sequence homology with c-Src, and has a similar domain arrangement, containing Src-homology 3 (SH3), Src-homology 2 (SH2), and kinase catalytic domains.<sup>2</sup> While c-Src has an N-terminal myristoylation site that targets the kinase to the cell membrane, Brk lacks a myristoylation sequence, and is localized in both the cytoplasm and nucleus.<sup>2</sup>

The SH2 and SH3 domains of Brk regulate enzyme activity in a similar manner to Src by forming intramolecular interactions with other regions of the protein.<sup>3</sup> The SH2 domain of

\*Corresponding Author: Department of Physiology and Biophysics, Basic Science Tower, T-6, School of Medicine, Stony Brook University, Stony Brook, NY 11794-8661. Tel.: 631-444-3533. Fax: 631-444-3432. todd.miller@stonybrook.edu.

#### Supporting Information

Three supplemental figures and legends. The Supporting Information is available free of charge on the ACS Publications website at DOI: 10.1021/acs.biochem.5b00303.

#### Notes

The authors declare no competing financial interest.

Src interacts with the C-terminal tail phosphorylated at Tyr 527.<sup>4,5</sup> Likewise, the SH2 domain of Brk binds to its C-terminal sequence when phosphorylated at the analogous tyrosine residue, Tyr 447.<sup>3</sup> The SH3 domain of Src binds to the proline-rich linker region between the SH2 domain and the kinase domain,<sup>4,5</sup> and the SH3 domain of Brk functions in a similar manner.<sup>3,6,7</sup> In Brk, as in Src, these interactions are autoinhibitory. Engagement of the SH2 or SH3 domains by ligands or substrates disrupts these intramolecular interactions, leading to autophosphorylation of Brk at tyrosine 342 within the activation loop of the kinase domain, and increased activity.<sup>3,6</sup> Dephosphorylation of the C-terminal tail also serves to release these autoinhibitory interactions.<sup>3</sup>

Brk was first identified in a tyrosine kinase screen of metastatic breast cancers. It was found to be overexpressed in two-thirds of breast cancer samples and cell lines.<sup>8</sup> Aberrant expression of Brk is observed in several other cancers including ovarian<sup>9</sup> and prostate cancers.<sup>10,11</sup> Overexpression of Brk in nonsmall cell lung cancer (NSCLC) is correlated to poor outcome.<sup>12</sup> Brk promotes cell proliferation through several signaling pathways. Brk increases proliferation of mammary epithelial cells in response to stimulation of epidermal growth factor (EGF)<sup>13,14</sup> through activation of the PI3K/Akt signaling pathway.<sup>13</sup> Brk activates ERK5 and p38-MAPK in response to EGF as well as heregulin.<sup>15</sup> Activation of signaling pathways is not limited to those downstream of the epidermal growth factor receptor family. Knockdown of Brk inhibits anchorage independent growth of cells induced by insulin-like growth factor 1 (IGF-1).<sup>16</sup> Brk is also critical for cell migration and may play a role in metastasis of cancer cells. Both p130Cas and paxillin have been identified as Brk substrates and phosphorylation of these substrates leads to increased cell migration.<sup>17,18</sup> Recently, Brk levels were found to be inversely correlated to E-cadherin levels, and targeting of Brk to the cell membrane of prostate epithelial cells promoted the epithelial to mesenchymal transition and increased metastasis of xenograft tumors.<sup>19</sup> Coexpression of Brk and ErbB2 decreased the sensitivity of cells to treatment with Lapatinib,<sup>20</sup> and expression of Brk in human mammary epithelial cells provides partial resistance to doxorubicin.<sup>21</sup> Together, these studies have identified Brk as a potential target for cancer therapy.

In addition to overexpression, tyrosine kinases can become hyperactivated in human cancer through somatic mutations. Activating mutations in the kinase domain of EGFR are a significant cause of NSCLC, and have been found to affect sensitivity of the kinase to small molecule inhibitors.<sup>22</sup> Mutations to c-Kit are observed in a significant proportion of gastrointestinal stromal tumors.<sup>23</sup> Jak3, a nonreceptor tyrosine kinase, is often mutated in T-cell acute lymphoblastic leukemia and other leukemias.<sup>24</sup> Several somatic mutations have been recently identified in the gene encoding PTK6/Brk. It has not been determined whether these cancer-associated mutations activate Brk or promote neoplastic growth.

In this study, we have examined a panel of Brk somatic mutations to assess enzymatic activity and substrate binding. The mutations were identified in different cancer types and are located across the different domains of Brk (Figure 1a). The L16F mutant, identified in clear cell renal cell carcinoma,<sup>25</sup> is found in the SH3 domain. The R131L mutant, found in gastric cancer,<sup>26</sup> is located in the SH2 domain. The V253M, N317S, and L343F mutants are found in the kinase domain. They were identified in head and neck squamous cell

carcinoma,<sup>27</sup> ovarian carcinoma,<sup>28</sup> and cutaneous squamous cell carcinoma,<sup>29</sup> respectively. The P450L mutant, identified in pancreatic cancer,<sup>30</sup> is located adjacent to the inhibitory tyrosine residue at the C-terminal tail of Brk. The location of these mutations suggests the possibility that the autoinhibitory interactions of Brk could be disrupted, leading to increased activity. We show that the L16F, R131L, L343F, and P450L mutations increase Brk activity, while the V253M and N317S mutants inactivate Brk. Furthermore, as the SH3 and SH2 domains also mediate substrate interactions, we observe mutant-specific effects on substrate binding and phosphorylation.

## MATERIALS AND METHODS

### Reagents and Antibodies

Bovine serum albumin (BSA) was obtained from Amresco. Leupeptin and aprotinin were from Roche. Phenylmethylsulfonyl fluoride, sodium vanadate, dithiothreitol (DTT), and Polybrene were from Sigma, and NAF was purchased from JT Baker. Human epidermal growth factor (EGF) was purchased from Millipore. Primary antibodies were obtained from the following companies: antiphospho-Akt (Ser473), anti-Akt, antiphospho-p130 Cas (Tyr249), antiphospho-p44/42 MAPK (Erk1/2) (Thr202/Tyr204) (D13.14.4E), p44/42 MAPK (Erk1/2), and antiphospho STAT3 (Tyr 705) were from Cell Signaling Technology, anti-ErbB2 (24B5), antiphospho Brk (Tyr342), antiphosphotyrosine, clone 4G10, were from Millipore, anti-p130 Cas (C-20), anti-Sam68 (c-20), anti-Stat3 (H-190), and anti-pTyr (pY99) were from Santa Cruz, anti- $\beta$ -catenin was from BD Biosciences, and monoclonal ANTI-FLAG M2-peroxidase (HRP) was from Sigma. Horseradish peroxidase linked donkey anti-rabbit IgG and sheep anti-mouse antibodies were from GE Healthcare. SuperSignal West Femto Chemiluminescent Substrate and Pierce ECL Western Blotting Substrate were purchased from Thermo Scientific.

### Cell Lines

The mammalian cell lines HEK293T, Src<sup>-</sup>Yes<sup>-</sup>Fyn<sup>-</sup> null (SYF), NIH-3T3, and SkBr3 were cultured in Dulbecco's modified Eagle's medium (Corning) with 10% fetal bovine serum (Seradigm) and 1000 units/mL penicillin, 1 mg/mL streptomycin, and 2.5  $\mu$ g/mL amphotericin B (Corning). 293-GPG cells used for generating retrovirus were maintained in DMEM with 10% FBS, 300  $\mu$ g/mL L-glutamine, 1 $\times$  penicillin/streptomycin solution (Corning), 100  $\mu$ g/mL tetracyclin (Sigma), 2  $\mu$ g/mL puromycin (Gibco), and 300  $\mu$ g/mL G418 (Corning). MCF-10a cells were maintained in DMEM/F12 (Corning) containing 5% horse serum (Sigma), 20 ng/mL EGF (Millipore), 0.5  $\mu$ g/mL hydrocortisone (MP Biomedical), 100 ng/mL cholera toxin, 10  $\mu$ g/mL insulin (Sigma), and 1 $\times$  penicillin/streptomycin (Corning). MCF-10a cells were starved in growth media with only 2% horse serum and without EGF.

### DNA Constructs and Mutagenesis

The baculovirus vector for His-tagged Brk and the mammalian expression vector for Flag-tagged Brk were described previously.<sup>3,6</sup> Site-directed mutagenesis was performed using the Stratagene QuikChange Kit, and mutations were confirmed by DNA sequencing. Full-length ErbB2 in pcDNA3.1-neo and Flag-tagged  $\beta$ -catenin in pcDNA3.1 mammalian expression

vectors were gifts from Drs. Deborah Brown and Dr. Ken-Ichi Takemaru, respectively, of Stony Brook University. The expression vector for p130Cas in pcDNA3.1/V5-His B was described previously.<sup>31</sup>

### Transient Transfection, Western Blotting, and Immunoprecipitation

Cells ( $1 \times 10^6$ ) were transfected 24 h after plating with 8  $\mu\text{L}$  of polyethylenimine per  $\mu\text{g}$  of DNA in 150 mM NaCl. Cells were harvested 48 h post-transfection using RIPA buffer (25 mM Tris, pH 7.5, 1 mM EDTA, 100 mM NaCl, 1% NP-40) supplemented with aprotinin, leupeptin, PMSF, NaF, DTT, and  $\text{Na}_3\text{VO}_4$ . The lysates were resolved by SDS-PAGE and transferred to PVDF membranes and probed with the appropriate antibodies, or were used in immunoprecipitation assays.

For immunoprecipitation studies, 1 mg/mL of cell lysate was precleared with 15  $\mu\text{L}$  of protein G agarose beads for 1 h at 4 °C on a rotator. The precleared lysates were incubated with 1  $\mu\text{g}$  of the appropriate antibody for 1 h at 4 °C, and then combined with 15  $\mu\text{L}$  of fresh protein G agarose for 4 h at 4 °C. The beads were washed three times with RIPA buffer, and then eluted with SDS-PAGE buffer and resolved by SDS-PAGE. The proteins were transferred to PVDF membrane for Western blot analysis.

For immunoprecipitation of Flag-tagged Brk, cell lysates (1 mg protein) were incubated with 45  $\mu\text{L}$  of anti-Flag M2 affinity gels (Sigma) on a rotator for 3 h at 4 °C, and then washed three times with Tris-buffered saline (TBS). The immunoprecipitated proteins were divided in three tubes. Duplicate samples were used for a radioactive kinase assay with Src peptide (sequence: AEEEEIYGEFEAKKKKG). The immunoprecipitated proteins were incubated with 15  $\mu\text{L}$  of reaction buffer (30 mM Tris, pH 7.5, 20 mM  $\text{MgCl}_2$ , 1 mg/mL BSA, 200  $\mu\text{M}$  ATP), 1.2 mM Src peptide, and 50–100 cpm/pmol of [ $\gamma^{32}\text{-P}$ ] ATP at 30 °C for 10 min. The reaction was quenched using 45  $\mu\text{L}$  of 10% trichloroacetic acid. The samples were centrifuged, and 30  $\mu\text{L}$  of the reaction was spotted onto Whatman P81 cellulose phosphate paper, which was washed with 0.5% phosphoric acid. Transfer of radioactive phosphate to the peptide was measured by scintillation counting.

### Peptide Binding Assay

SH2 ligand peptide (ETpYEEYGYDG) or SH3 ligand peptide (RGAAPPPPVPRGRG) were coupled to Affi-gel 15 resin (Biorad) by incubation in 0.1 M Hepes (pH 7.5) overnight at 4 °C. Unreacted resin was then blocked with 100 mM ethanolamine. The peptide conjugated beads were washed with 0.1 M Hepes (pH 7.5) then equilibrated with binding buffer (5 mM EDTA, 50 mM Tris, pH 7.5, 100 mM NaCl, 0.1% Triton X-100, 1 mM DTT, 0.5 mM  $\text{Na}_3\text{VO}_4$ ). Lysates (500  $\mu\text{g}$ ) from transiently transfected cells were incubated with the beads for 1 h at 4 °C. The bound protein was eluted with SDS-PAGE sample buffer, resolved by SDS-PAGE, and analyzed by Western blotting.

### Stable Cell Expression

The MSCV-PIG vector and 293-GPG cells were a kind gift from Dr. Senthil Muthuswamy (University of Toronto). To generate retrovirus, 15  $\mu\text{g}$  of DNA was combined with 50  $\mu\text{L}$  of Lipofectamine 2000 (Life Technologies) in 2 mL of serum-free DMEM. The mixture was

added to 293-GPG cells in 4 mL of fresh serum-free DMEM. Following a 6 h incubation, 5 mL of fresh media was added to the cells, and incubation continued overnight. The media was replaced the following day. Virus collected on the fifth day after transfection was filtered with a 0.45  $\mu\text{m}$  filter and combined with 4 mL of media and 8  $\mu\text{g}/\text{mL}$  Polybrene and added to NIH-3T3 cells. Following a 5 h incubation, 6 mL of fresh media was added to the cells. Puromycin (2  $\mu\text{g}/\text{mL}$ ) was added to the cells 48 h postinfection to select for positively infected cells. Stable cells were monitored by GFP expression.

### Growth Assays

Cells (20 000) were plated in duplicate in 12-well plates. At each time point, the cells were trypsinized, then resuspended in media and counted with a hemocytometer. To measure nonanchored cell growth, 20 000 cells were plated in triplicate in 24-well low attachment plates (Corning). On day 6, the cells were centrifuged then resuspended using 100  $\mu\text{L}$  of trypsin and counted with a hemocytometer.

### Migration Assay

MCF-10a cells were serum starved overnight, and plated in duplicate into 24-well Transwell plates with 0.8  $\mu\text{m}$  polyester inserts (Corning). Media with or without EGF was added to the bottom chamber. After 8 h, nonmigrated cells were swabbed from the top of the chamber and the migrated cells were fixed with formaldehyde and stained with DAPI. Cells were counted and averaged for 5 different areas of each well.

### Isothermal Titration Calorimetry

The pET28 SAC SP vector encoding the Brk SH2 domain was a kind gift from Dr. John Engen (Northeastern University). The SH2 domain was expressed in BL21 (DE3) *E. coli* cells. Cells were lysed in a French pressure cell, and the SH2 domain was purified by chromatography on NiNTA agarose. Purified protein was dialyzed overnight in ITC buffer (20 mM Hepes, 1 mM EDTA, 250 mM NaCl, 1 mM  $\beta$ -mercaptoethanol, and 5% glycerol). Synthetic peptides based on the wild-type or mutant Brk C-terminal tail were from Genemed Synthesis, Inc. Crude peptides were purified by reverse-phase HPLC and dialyzed in ITC buffer. The protein was diluted to 67.4  $\mu\text{M}$  and the wild-type (FTS-Y(p)-ENLTG) and P450L (FTS-Y(p)-ENPTG) peptides were diluted to 1 mM and 827  $\mu\text{M}$ , respectively. The protein and peptides were degassed at 4  $^{\circ}\text{C}$  and loaded into the sample cell and syringe, respectively. ITC experiments were performed on a MicroCal VP-ITC microcalorimeter at 25  $^{\circ}\text{C}$  with 5  $\mu\text{L}$  of peptide added per injection. Origin 7.0 was used for data fitting.

## RESULTS

### Cancer-Associated Mutations Affect Brk Activity

We introduced the six mutations into expression vectors encoding Flag-tagged full length Brk and expressed the proteins in HEK293T cells. We measured Brk phosphorylation in cell lysates using a general phosphotyrosine antibody and with an antibody specific for pY342, the major site of autophosphorylation in Brk.<sup>3</sup> The mutations located within important regulatory regions of Brk, L16F (SH3), R131L (SH2), and P450L (adjacent to the regulatory C-terminal phosphotyrosine), caused significant increases in Brk autophosphorylation

(Figure 1B). The L343F mutant, which is adjacent to the autophosphorylation site in the activation loop, also increased phosphorylation of tyrosine 342. The V253M and N317S mutations in the Brk kinase domain reduced autophosphorylation activity to undetectable levels. An additional anti-phosphotyrosine Western blot, showing higher-molecular weight proteins, is presented in Supporting Information Figure 1. To confirm activation of Brk, we immunoprecipitated Brk from cell lysates and incubated the protein with a synthetic peptide substrate in the presence of [ $\gamma^{32}$ -P] ATP. The mutants that showed increased autophosphorylation also had increased activity against the peptide, although the degree of activation toward the exogenous substrate was not as high (Figure 1c). The N317S mutant was inactive in this assay, consistent with its lack of autophosphorylation (Figure 1B).

### Cancer-Associated Mutations Disrupt Brk Intermolecular and Intramolecular Interactions

The P450L mutation is located at the P+3 position relative to the regulatory tyrosine (Y447) at the Brk C-terminal tail. The identity of the amino acid at the P+3 position often dictates the affinity and specificity of SH2 ligands;<sup>32</sup> thus, the P450L mutation could potentially affect autoinhibitory binding between the Brk SH2 domain and phosphorylated Y447. We tested this possibility first with a peptide affinity assay, using a peptide containing the pYEEY sequence that we previously showed binds to the SH2 domain of Brk.<sup>6</sup> The autoinhibited forms of Src and Brk bind weakly to immobilized SH2 ligands because their SH2 domains are engaged with their phosphorylated C-terminal tails, while activated forms bind more strongly.<sup>3,33</sup> We incubated the immobilized pYEEY peptide with lysates from cells expressing wild-type or P450L Brk. The P450L mutant showed increased affinity for the SH2 ligand compared to wild-type Brk (Figure 1d), suggesting that the P450L mutation may disrupt the inhibitory interaction between the SH2 domain and the C-terminal tail of Brk. We also measured binding of the SH2 domain to a synthetic peptide based on the phosphorylated C-terminal tail of Brk (FTSpYENPTG) or to a similar peptide containing the P450L substitution (FTSpYENLPTG) by isothermal titration calorimetry. The dissociation constant of the Brk SH2 domain for a phosphorylated Brk C-terminal tail peptide increased from 15  $\mu$ M to 53  $\mu$ M with the introduction of the P450L mutation (Supporting Information Figure 2). This is consistent with a decreased interaction between the SH2 domain and its phosphorylated C-terminal tail in the Brk P450L mutant.

Based on the autoinhibited structure of Src kinases, the Brk SH3 domain is predicted to bind to the SH2-kinase linker to stabilize the autoinhibited conformation. Mutations within the linker sequence strongly activate Brk.<sup>6</sup> A structural analysis of the Brk SH3 domain showed that Trp17 (the residue adjacent to Leu16) interacts with Pro179 in the linker region.<sup>34</sup> Thus, activation of Brk by the L16F mutation (Figure 1B) could be due to the disruption of SH3-linker interactions. The SH3 domain of Brk plays a key role in the recognition of substrates, so the L16F mutation could also interfere with substrate binding. We carried out a binding assay using an immobilized peptide based on the SH3 recognition sequence on Sam68, a physiological substrate of Brk. The L16F mutant showed decreased binding to the SH3 ligand compared to wild-type Brk, which suggests that the ability of the L16F mutant to recognize its substrates would be compromised (Figure 1D).

## Effect of Brk Mutants on Cell Growth

Several studies have supported a role for Brk as an oncogenic driver of cancer. Expression of Brk increases cell proliferation and promotes anchorage independent growth,<sup>14</sup> a measure of transforming potential. Brk also promotes tumorigenesis in the mouse mammary gland,<sup>35</sup> and decreases tumor latency.<sup>21</sup> Knock-down of Brk inhibits cell growth.<sup>15,36</sup> We measured anchored and nonanchored growth of NIH-3T3 cells stably expressing wild-type Brk or the cancer-associated mutants. We expressed Brk using a retroviral vector that contains an internal ribosomal entry site for expression of GFP. We selected Brk expressing cells by puromycin treatment, and analyzed cells with equivalent GFP expression. Cells expressing wild-type Brk showed increased cell growth compared to empty vector cells, with the greatest difference in cell number at Day 6 (Figure 2A). All of the stable cells expressing Brk mutants showed reduced proliferation relative to wild-type Brk, and cells that expressed the P450L mutant did not survive past Day 6. We examined anchorage-independent growth using plates with a neutral surface to minimize cell attachment. We observed an increase in nonanchored growth in NIH3T3 cells expressing wild-type Brk as compared to control cells, but there were no significant differences between control cells and cells expressing Brk mutants (Figure 2B).

The effect of Brk expression on cell growth is most often studied in the context of breast cancer. We stably expressed wild-type or mutant forms of Brk in MCF-10a nontransformed mammary epithelial cells, as well as in SKBR3 cells, which are a transformed mammary cell line. We chose the SKBR3 cell line because it overexpresses ErbB2, which we have previously shown to cooperate with Brk to enhance cell growth.<sup>20</sup> Similarly to the results in NIH3T3 cells, MCF-10a cells expressing the P450L and L16F mutants showed reduced proliferation relative to wild-type Brk (Figure 3). In SKBr3 cells, we observed no difference in proliferation between control cells and cells expressing Brk (wild-type or mutant) at Day 6 (data not shown) or Day 14 (Supporting Information Figure 3).

## Effect of Brk Mutants on Signaling Pathways

Several of the cancer-associated mutations increased Brk activity, yet reduced cell growth. To understand the basis for these effects, we examined signaling pathways that are often activated in cancer. Brk is a mediator of signaling downstream of the EGFR family of receptor kinases. Coexpression of Brk with ErbB2 leads to increase in phosphorylation of Erk1/2.<sup>20</sup> We first examined the effect of two of the mutations (L16F and P450L) on interaction with the ErbB2 receptor. Activation of ErbB2 leads to transphosphorylation of the intracellular domain, which provides binding sites for cellular proteins containing SH2 domains, including Brk.<sup>37</sup> Mutations to Brk that interfere with inhibitory intramolecular interactions could allow greater access of Brk to the SH2 binding sites. We cotransfected ErbB2 and Brk into 293T cells, immunoprecipitated ErbB2, and examined Brk association by Western blotting. The L16F and P450L mutants showed increased interaction with ErbB2 compared to wild-type Brk (Figure 4A).

Akt kinase has previously been identified as a binding partner and substrate for Brk.<sup>38</sup> We did not observe any differences in Akt phosphorylation between control 293T cells or cells expressing WT or mutant forms of Brk (Figure 4B). The L16F mutant showed increased

phosphorylation of Erk1/2 compared to wild-type Brk (Figure 4B). In serum starved cells, no phosphorylation of Erk1/2 was observed, and there was no appreciable difference between wild-type and L16F Brk following stimulation with EGF (Figure 4C). This suggests that the L16F mutation disrupts autoinhibitory constraints in Brk, but does not activate Brk to levels higher than those achieved by EGF stimulation. The increased phosphorylation of Erk1/2 by the L16F mutant in cells that were not serum starved (Figure 4B) suggests that the L16F mutant may be more sensitive to activation by other factors. Akt and Erk1/2 were still phosphorylated in cells expressing the catalytically inactive N317S mutant, suggesting that this mutant might potentiate phosphorylation of signaling molecules by another kinase (e.g., a Src family kinase), perhaps by acting as a scaffolding protein. These results are consistent with observations of cell migration and cell growth upon expression of kinase inactive Brk.<sup>36,39</sup> We also measured activation of Akt and Erk1/2 in SkBr3 breast cancer cells (Supporting Information Figure 3). We observed increased activation of both Akt and Erk1/2 in cells expressing the L343F mutant, but there was no increase in anchored or nonanchored cell growth.

A number of Brk substrates and interacting proteins have been identified in normal epithelial cells, as well as in tumors.<sup>40</sup> p130 CRK-associated substrate (Cas) is a substrate of Brk that is localized to focal adhesions and acts as an adaptor protein to facilitate cell migration.<sup>41</sup> Cas has been shown to be a direct substrate of Brk and mediates Brk-induced cell migration of prostate cells.<sup>17</sup> We cotransfected 293T cells with Brk and Cas, and probed the cell lysates with a phospho-specific Cas antibody (pY165). The R131L, L343F, and P450L mutants all showed greater phosphorylation of Cas compared to wild-type Brk (Figure 4D). The L16F mutant showed decreased phosphorylation of Cas. This may be partly due to decreased expression of L16F Brk upon coexpression with Cas, an effect we observed consistently. Additionally or alternatively, decreased phosphorylation of Cas by the L16F mutant could result from decreased binding between the proteins. Src interacts with Cas through its SH3 domain.<sup>42</sup> The L16F mutation is within the SH3 domain of Brk and interferes with ligand binding (Figure 1); thus, the mutation may disrupt the Brk-Cas interaction.

The transcription factor, signal transducer and activator of transcription 3 (STAT3), is a substrate for Brk.<sup>43</sup> Constitutive activation of STAT3 has been observed in many types of cancer. Phosphorylation of STAT3 by Brk increases its transcriptional activity and coexpression of STAT3 and Brk promote cell proliferation.<sup>43</sup> We observed a decrease in phosphorylation of STAT3 in cells expressing the V253M and N317S mutants compared to control cells or cells expressing wild-type Brk (Figure 4e), suggesting that these mutants may exert a dominant-negative effect on STAT3 phosphorylation.

Sam68, an RNA binding protein, was one of the first substrates identified for Brk. Sam68 is upregulated in breast cancer<sup>44</sup> and prostate cancer,<sup>45</sup> and expression of Brk relocalizes Sam68 to Sam68-SLM nuclear bodies (SNBs),<sup>46</sup> which are often observed in cancer cells.<sup>47</sup> We transiently expressed Brk (wild-type or mutants) in 293T cells, immunoprecipitated endogenous Sam68, and examined phosphorylation by SDS-PAGE and antiphosphotyrosine Western blotting. We also probed the membranes with Flag antibody to measure association of Brk. The R131L, L343F, and P450L mutants showed a small increase in Sam68 binding



and phosphorylation compared to wild-type Brk (Figure 4F). While the L16F mutant increased Brk activity (Figure 1), there was decreased binding and phosphorylation of Sam68 by this mutant compared to WT Brk (Figure 4F). This is likely due to the effect of the L16F mutation on the ligand-binding ability of the SH3 domain (Figure 1D), which is critical for interaction with Sam68.<sup>6,48</sup> The N317S mutation, which drastically reduced autophosphorylation (Figure 1B), severely compromised Sam68 binding and tyrosine phosphorylation (Figure 4F).

Phosphorylation of  $\beta$ -catenin by Brk inhibits its transcriptional activity.<sup>49</sup> We measured phosphorylation of  $\beta$ -catenin in cells coexpressing  $\beta$ -catenin and wild-type or mutant forms of Brk. We immunoprecipitated  $\beta$ -catenin from the lysates and probed with a general phosphotyrosine antibody. We reprobed the membrane with Flag antibody to assess Brk association. The R131L, L343F, and P450L mutants all showed greater binding and phosphorylation of  $\beta$ -catenin as compared to wild-type Brk (Figure 4G). The L16F mutant was not able to phosphorylate  $\beta$ -catenin, likely due to its decreased interaction with the protein (Figure 4G). While the N317S mutant bound normally to  $\beta$ -catenin, it was unable to phosphorylate the protein. The results suggest that increased phosphorylation of  $\beta$ -catenin by several of the cancer-associated mutants could underlie the reduced cell growth observed in NIH3T3 and MCF-10a cells.

## DISCUSSION

Tyrosine kinases have emerged as one of the most frequently mutated gene families in cancer.<sup>50,51</sup> In some cases (e.g., EGF receptor and c-Kit), the mutant kinases have increased enzymatic activity and transforming ability.<sup>52</sup> Brk was originally identified as a gene that is overexpressed in metastatic breast cancer, and several studies have supported a role for Brk as a driver of tumorigenesis. Brk is a key mediator in several signaling pathways, functioning downstream from the EGFR family of receptors<sup>13–15,53</sup> as well as IGF1R.<sup>16</sup> Aberrant expression of Brk promotes cell growth and migration, and the epidermal to mesenchymal transition<sup>19</sup> and is involved in hypoxia induced growth in breast cancer.<sup>54</sup> Sequencing efforts to fully identify the genetic landscape of different cancers have revealed several cancer-associated mutations to Brk. It has not been determined whether these mutations are driver mutations that are critical for oncogenesis, or simply passenger mutations that do not contribute any growth advantage. In this study, we have shown that the L16F, R131L, L343F, and P450L mutants activate Brk as determined by autophosphorylation. The activation of Brk was corroborated by measuring the phosphorylation of a synthetic peptide substrate. In contrast, the V253M and N317S mutations eliminate the catalytic activity of Brk. The effects of the mutants are summarized in Table 1.

The P450L and L16F mutations are predicted to affect intramolecular and intermolecular interactions of Brk. Our results suggest that the P450L mutation weakens binding between the SH2 domain and the C-terminal tail, an important interaction for maintaining Brk in its autoinhibited conformation; the mutation concomitantly increases accessibility of the SH2 domain for interaction with various substrates (Figures 1D and 4, and Supporting Information Figure 2). The L16F mutation leads to decreased interaction with an SH3 ligand

(Figure 1D). The L16F mutation activated Brk (Figure 1B) and promoted phosphorylation of Erk1/2 (Figure 4F), but dramatically decreased the ability of Brk to bind and phosphorylate other substrates such as Sam68 and  $\beta$ -catenin. (Figure 4F,G). This supports previous studies that showed the SH3 domain is essential for interaction with Sam68,<sup>6</sup> and highlights the importance of this domain for interaction with  $\beta$ -catenin. This mutation may also inhibit interaction with other substrates such as paxillin, which Brk also phosphorylates to promote cell migration. Both the SH2 and SH3 domains were shown to be involved in interaction with paxillin.<sup>18</sup>

The V253M and N317S mutations inactivate Brk (Figure 1B,C) and expression of the N317S mutant in cells inhibits phosphorylation of several substrates including Sam68 and  $\beta$ -catenin (Figure 4). Erk1/2 and Akt are still phosphorylated in cells expressing the N317S mutant (Figure 4). These results show that the catalytic activity is important for activation of Sam68 and  $\beta$ -catenin, but imply that a catalytically inactive form of Brk is able to facilitate phosphorylation of other substrates. Previous studies have shown that a kinase-dead mutant of Brk is still able to promote proliferation of T-47D breast cancer cells,<sup>36</sup> consistent with these observations. Additionally, recent studies in several cancer types have shown a correlation between decreased expression of Brk and poor prognosis.<sup>55-57</sup> Loss-of-function mutations in Brk could potentially disrupt its function as a tumor suppressor.

Expression of wild-type Brk showed an increase in anchored and nonanchored cell growth, as previously observed.<sup>14,21,35</sup> While several of the mutations increased Brk kinase activity, expression unexpectedly led to decreased cell proliferation (Figures 2 and 3, and Supporting Information Figure 3). We hypothesize that this effect may be due to differential interaction and activation of Brk substrates. We observed an increase in the interactions of the L16F and P450L mutants with ErbB2, relative to WT Brk (Figure 4A). We have previously shown that coexpression of Brk and ErbB2 promotes cell proliferation mainly through activation of the Ras-MAPK pathway.<sup>20</sup> Thus, activation of Brk and increased interaction with ErbB2 by the L16F and P450L mutants would be expected to result in increased phosphorylation of Erk1/2, and potentially Akt, which is another key signaling protein downstream of ErbB2 and is a substrate of Brk.<sup>13,38</sup> The L16F mutant (but not the P450L mutant) showed an increase in activation of Erk1/2, and we observed no significant difference between mutants compared to wild-type Brk for the activation of Akt. The lack of Akt activation by L16F Brk may be due to interference with SH3 ligand binding; the SH3 domain of Brk is important for interaction with Akt.<sup>38</sup>

Differential phosphorylation of Brk substrates could result in activation of both pro- and antiproliferative pathways. Activation of  $\beta$ -catenin has been implicated in colon cancer and NSCLC.<sup>58</sup> Expression of the R131L, L343F, and P450L mutants led to increased phosphorylation of  $\beta$ -catenin (Figure 4G). Phosphorylation of  $\beta$ -catenin by Brk inhibits transcriptional activity.<sup>49</sup> Coexpression of an alternatively spliced variant of Brk (Alt-PTK6) enhances Brk downregulation of  $\beta$ -catenin and decreases colony formation of a prostate adenocarcinoma cell line.<sup>59</sup> Thus, the enhanced phosphorylation of  $\beta$ -catenin by the Brk mutants could partially explain the decrease in proliferation.

Whether Brk and Sam68 cooperate in a pro- or antitumorigenic manner is less clear. Sam68 may contribute to oncogenesis by promoting alternative splicing. For example, Sam68 promotes inclusion of a variable exon 5 in the *CD44* pre-mRNA, which is correlated with tumorigenesis.<sup>45</sup> Furthermore, expression of an RNA-binding deficient Sam68 inhibits cell growth.<sup>45</sup> When phosphorylated by Brk, Sam68 relocates to distinct nuclear bodies (SNBs) in breast and colon cancer cells; the presence of SNBs is correlated with tumorigenicity in some cancers.<sup>46</sup> On the other hand, phosphorylation of Sam68 by Brk inhibits its RNA-binding activity.<sup>48</sup> The R131L, L343F, and P450L mutants increased phosphorylation of Sam68 (Figure 4F); thus, expression of the mutants may inhibit the RNA-binding activity of Sam68 which is important for cell growth.

The localization of Brk is an additional factor that can modulate its tumorigenic potential. Brk lacks an N-terminal myristoylation sequence, which is important for membrane association in Src family kinases,<sup>2</sup> and it also lacks a nuclear localization sequence.<sup>40</sup> In poorly differentiated prostate cell lines such as PC3, which form aggressive tumors in animals, Brk is mainly found in the cytoplasm.<sup>10</sup> Targeting of Brk to the cell membrane promotes cell growth and transformation.<sup>60</sup> We have shown that cancer-associated mutations can affect the interaction of Brk with its substrates, which may have indirect effects on the subcellular localization of the kinase.

In summary, we have shown for the first time that cancer-associated mutations can affect Brk activity. Several of the mutations activate Brk, while the V253M and N317S mutations drastically reduce kinase activity. We have also shown that the mutations alter the set of substrates Brk is able to bind and phosphorylate, which may result in both positive and negative signals for cell growth and transformation. Expression of the mutants decreased cell proliferation, but did not result in overt changes in transformation (as measured by nonanchored cell growth) or migration in the cell systems we studied (Figures 3 and 4, and Supporting Information Figure 3). The tissues in which these mutations arose could contain a different collection, or a different balance, of signaling components. Thus, Brk mutations could contribute to tumorigenesis by different mechanisms in different cell contexts. Cancer-associated somatic mutations can have important consequences in tumor growth and drug resistance. Because there is currently no reliable method to predict the consequence of somatic mutations, experimental testing and validation is essential.

## Supplementary Material

Refer to Web version on PubMed Central for supplementary material.

## Acknowledgments

We thank Jincy Mathew for assistance with site-directed mutagenesis of Brk.

**Funding:** This work was supported by National Institutes of Health Grant CA58530 to W.T.M.

## ABBREVIATIONS

**Brk** breast tumor kinase

<b>PTK6</b>	protein tyrosine kinase 6
<b>Frk</b>	fyn-related Src family tyrosine kinase
<b>Srms</b>	Src-related kinase lacking C-terminal regulatory tyrosine and N-terminal myristoylation sites
<b>Sik</b>	Src-related intestinal kinase
<b>SH2</b>	Srchomology 2
<b>SH3</b>	Src-homology 3
<b>NSCLC</b>	nonsmall cell lung cancer
<b>Erk5</b>	extracellular-signal-regulated kinase 5
<b>MAPK</b>	mitogen-activated protein kinase
<b>IGF-1</b>	insulin-like growth factor I
<b>IGF1R</b>	insulin-like growth factor I receptor
<b>Cas</b>	Crk-associated substrate
<b>EGFR</b>	epidermal growth factor receptor
<b>BSA</b>	bovine serum albumin
<b>DTT</b>	dithiothreitol
<b>STAT3</b>	signal transducer and activator of transcription 3

## References

1. Serfas MS, Tyner AL. Brk, Srm, Frk, and Src42A form a distinct family of intracellular Src-like tyrosine kinases. *Oncol Res.* 2003; 13:409–419. [PubMed: 12725532]
2. Mitchell PJ, Barker KT, Martindale JE, Kamalati T, Lowe PN, Page MJ, Gusterson BA, Crompton MR. Cloning and characterisation of cDNAs encoding a novel non-receptor tyrosine kinase, brk, expressed in human breast tumours. *Oncogene.* 1994; 9:2383–2390. [PubMed: 8036022]
3. Qiu H, Miller WT. Regulation of the nonreceptor tyrosine kinase Brk by autophosphorylation and by autoinhibition. *J Biol Chem.* 2002; 277:34634–34641. [PubMed: 12121988]
4. Xu W, Harrison SC, Eck MJ. Three-dimensional structure of the tyrosine kinase c-Src. *Nature.* 1997; 385:595–602. [PubMed: 9024657]
5. Bjorge JD, Jakymiw A, Fujita DJ. Selected glimpses into the activation and function of Src kinase. *Oncogene.* 2000; 19:5620–5635. [PubMed: 11114743]
6. Qiu H, Miller WT. Role of the Brk SH3 domain in substrate recognition. *Oncogene.* 2004; 23:2216–2223. [PubMed: 14676834]
7. Kim H, Jung J, Lee ES, Kim YC, Lee W, Lee ST. Molecular dissection of the interaction between the SH3 domain and the SH2-Kinase Linker region in PTK6. *Biochem Biophys Res Commun.* 2007; 362:829–834. [PubMed: 17822667]
8. Barker KT, Jackson LE, Crompton MR. BRK tyrosine kinase expression in a high proportion of human breast carcinomas. *Oncogene.* 1997; 15:799–805. [PubMed: 9266966]
9. Schmandt RE, Bennett M, Clifford S, Thornton A, Jiang F, Broaddus RR, Sun CC, Lu KH, Sood AK, Gershenson DM. The BRK tyrosine kinase is expressed in high-grade serous carcinoma of the ovary. *Cancer Biology & Therapy.* 2006; 5:1136–1141. [PubMed: 16855388]

10. Derry JJ, Prins GS, Ray V, Tyner AL. Altered localization and activity of the intracellular tyrosine kinase BRK/Sik in prostate tumor cells. *Oncogene*. 2000; 22:4212–4220. [PubMed: 12833144]
11. Zheng Y, Tyner AL. Context-specific protein tyrosine kinase 6 (PTK6) signalling in prostate cancer. *Eur J Clin Invest*. 2013; 43:397–404. [PubMed: 23398121]
12. Zhao C, Chen Y, Zhang W, Zhang J, Xu Y, Li W, Chen S, Deng A. Expression of protein tyrosine kinase 6 (PTK6) in nonsmall cell lung cancer and their clinical and prognostic significance. *Onco Targets Ther*. 2013; 6:183–188. [PubMed: 23525678]
13. Kamalati T, Jolin HE, Fry MJ, Crompton MR. Expression of the BRK tyrosine kinase in mammary epithelial cells enhances the coupling of EGF signalling to PI 3-kinase and Akt, via erbB3 phosphorylation. *Oncogene*. 2000; 19:5471–5476. [PubMed: 11114724]
14. Kamalati T, Jolin HE, Mitchell PJ, Barker KT, Jackson LE, Dean CJ, Page MJ, Gusterson BA, Crompton MR. Brk, a Breast Tumor-derived Non-receptor Protein-tyrosine Kinase, Sensitizes Mammary Epithelial Cells to Epidermal Growth Factor. *J Biol Chem*. 1996; 271:30956–30963. [PubMed: 8940083]
15. Ostrander JH, Daniel AR, Lofgren K, Kleer CG, Lange CA. Breast tumor kinase (protein tyrosine kinase 6) regulates heregulin-induced activation of ERK5 and p38 MAP kinases in breast cancer cells. *Cancer Res*. 2007; 67:4199–4209. [PubMed: 17483331]
16. Irie HY, Shrestha Y, Selfors LM, Frye F, Iida N, Wang Z, Zou L, Yao J, Lu Y, Epstein CB, Natesan S, Richardson AL, Polyak K, Mills GB, Hahn WC, Brugge JS. PTK6 regulates IGF-1-induced anchorage-independent survival. *PLoS One*. 2010; 5:e11729. [PubMed: 20668531]
17. Zheng Y, Asara JM, Tyner AL. Protein-tyrosine kinase 6 promotes peripheral adhesion complex formation and cell migration by phosphorylating p130 CRK-associated substrate. *J Biol Chem*. 2012; 287:148–158. [PubMed: 22084245]
18. Chen HY, Shen CH, Tsai YT, Lin FC, Huang YP, Chen RH. Brk activates rac1 and promotes cell migration and invasion by phosphorylating paxillin. *Mol Cell Biol*. 2004; 24:10558–10572. [PubMed: 15572663]
19. Zheng Y, Wang Z, Bie W, Brauer PM, Perez White BE, Li J, Nogueira V, Raychaudhuri P, Hay N, Tonetti DA, Macias V, Kajdacsy-Balla A, Tyner AL. PTK6 activation at the membrane regulates epithelial-mesenchymal transition in prostate cancer. *Cancer Res*. 2013; 73:5426–5437. [PubMed: 23856248]
20. Xiang B, Chatti K, Qiu H, Lakshmi B, Krasnitz A, Hicks J, Yu M, Miller WT, Muthuswamy SK. Brk is coamplified with ErbB2 to promote proliferation in breast cancer. *Proc Natl Acad Sci U S A*. 2008; 105:12463–12468. [PubMed: 18719096]
21. Lofgren KA, Ostrander JH, Housa D, Hubbard GK, Locatelli A, Bliss RL, Schwertfeger KL, Lange CA. Mammary gland specific expression of Brk/PTK6 promotes delayed involution and tumor formation associated with activation of p38 MAPK. *Breast Cancer Res*. 2011; 13:R89. [PubMed: 21923922]
22. Eck MJ, Yun CH. Structural and mechanistic underpinnings of the differential drug sensitivity of EGFR mutations in non-small cell lung cancer. *Biochim Biophys Acta*. 2010; 1804:559–566. [PubMed: 20026433]
23. Ma YY, Yu S, He XJ, Xu Y, Wu F, Xia YJ, Guo K, Wang HJ, Ye ZY, Zhang W, Tao HQ. Involvement of c-KIT mutation in the development of gastrointestinal stromal tumors through proliferation promotion and apoptosis inhibition. *Onco Targets Ther*. 2014; 7:637–643. [PubMed: 24833907]
24. Degryse S, de Bock CE, Cox L, Demeyer S, Gielen O, Mentens N, Jacobs K, Geerdens E, Gianfelici V, Hulselmans G, Fiers M, Aerts S, Meijerink JP, Tousseyn T, Cools J. JAK3 mutants transform hematopoietic cells through JAK1 activation, causing T-cell acute lymphoblastic leukemia in a mouse model. *Blood*. 2014; 124:3092–3100. [PubMed: 25193870]
25. Dalgliesh GL, Furge K, Greenman C, Chen L, Bignell G, Butler A, Davies H, Edkins S, Hardy C, Latimer C, Teague J, Andrews J, Barthorpe S, Beare D, Buck G, Campbell PJ, Forbes S, Jia M, Jones D, Knott H, Kok CY, Lau KW, Leroy C, Lin ML, McBride DJ, Maddison M, Maguire S, McLay K, Menzies A, Mironenko T, Mulderrig L, Mudie L, O'Meara S, Pleasance E, Rajasingham A, Shepherd R, Smith R, Stebbings L, Stephens P, Tang G, Tarpey PS, Turrell K, Dykema KJ, Khoo SK, Petillo D, Wondergem B, Anema J, Kahnoski RJ, Teh BT, Stratton MR,

- Futreal PA. Systematic sequencing of renal carcinoma reveals inactivation of histone modifying genes. *Nature*. 2010; 463:360–363. [PubMed: 20054297]
26. Zang ZJ, Ong CK, Cutcutache I, Yu W, Zhang SL, Huang D, Ler LD, Dykema K, Gan A, Tao J, Lim S, Liu Y, Futreal PA, Grabsch H, Furge KA, Goh LK, Rozen S, Teh BT, Tan P. Genetic and Structural Variation in the Gastric Cancer Kinome Revealed through Targeted Deep Sequencing. *Cancer Res*. 2011; 71:29–39. [PubMed: 21097718]
27. Stransky N, Egloff AM, Tward AD, Kostic AD, Cibulskis K, Sivachenko A, Kryukov GV, Lawrence MS, Sougnez C, McKenna A, Shefler E, Ramos AH, Stojanov P, Carter SL, Voet D, Cortes ML, Auclair D, Berger MF, Saksena G, Guiducci C, Onofrio RC, Parkin M, Romkes M, Weissfeld JL, Seethala RR, Wang L, Rangel-Escareno C, Fernandez-Lopez JC, Hidalgo-Miranda A, Melendez-Zajgla J, Winckler W, Ardlie K, Gabriel SB, Meyerson M, Lander ES, Getz G, Golub TR, Garraway LA, Grandis JR. The mutational landscape of head and neck squamous cell carcinoma. *Science*. 2011; 333:1157–1160. [PubMed: 21798893]
28. Bell D, et al. Integrated genomic analyses of ovarian carcinoma. *Nature*. 2011; 474:609–615. [PubMed: 21720365]
29. Durinck S, Ho C, Wang NJ, Liao W, Jakkula LR, Collisson EA, Pons J, Chan SW, Lam ET, Chu C, Park K, Hong S-w, Hur JS, Huh N, Neuhaus IM, Yu SS, Grekin RC, Mauro TM, Cleaver JE, Kwok PY, LeBoit PE, Getz G, Cibulskis K, Aster JC, Huang H, Purdom E, Li J, Bolund L, Arron ST, Gray JW, Spellman PT, Cho RJ. Temporal Dissection of Tumorigenesis in Primary Cancers. *Cancer Discovery*. 2011; 1:137–143. [PubMed: 21984974]
30. Kubo T, Kuroda Y, Kokubu A, Hosoda F, Arai Y, Hiraoka N, Hirohashi S, Shibata T. Resequencing analysis of the human tyrosine kinase gene family in pancreatic cancer. *Pancreas*. 2009; 38:e200–206. [PubMed: 19893451]
31. Patwardhan P, Shiba K, Gordon C, Craddock BP, Tamiko M, Miller WT. Synthesis of functional signaling domains by combinatorial polymerization of phosphorylation motifs. *ACS Chem Biol*. 2009; 4:751–758. [PubMed: 19627099]
32. Songyang Z, Cantley LC. Recognition and specificity in protein tyrosine kinase-mediated signalling. *Trends Biochem Sci*. 1995; 20:470–475. [PubMed: 8578591]
33. LaFevre-Bernt M, Sicheri F, Pico A, Porter M, Kuriyan J, Miller WT. Intramolecular regulatory interactions in the Src family kinase Hck probed by mutagenesis of a conserved tryptophan residue. *J Biol Chem*. 1998; 273:32129–32134. [PubMed: 9822689]
34. Ko S, Ahn KE, Lee YM, Ahn HC, Lee W. Structural basis of the auto-inhibition mechanism of nonreceptor tyrosine kinase PTK6. *Biochem Biophys Res Commun*. 2009; 384:236–242. [PubMed: 19401189]
35. Peng M, Ball-Kell SM, Franks RR, Xie H, Tyner AL. Protein tyrosine kinase 6 regulates mammary gland tumorigenesis in mouse models. *Oncogenesis*. 2013; 2:e81. [PubMed: 24323291]
36. Harvey AJ, Crompton MR. Use of RNA interference to validate Brk as a novel therapeutic target in breast cancer: Brk promotes breast carcinoma cell proliferation. *Oncogene*. 2003; 22:5006–5010. [PubMed: 12902983]
37. Dankort DL, Wang Z, Blackmore V, Moran MF, Muller WJ. Distinct tyrosine autophosphorylation sites negatively and positively modulate neu-mediated transformation. *Mol Cell Biol*. 1997; 17:5410–5425. [PubMed: 9271418]
38. Zheng Y, Peng M, Wang Z, Asara JM, Tyner AL. Protein tyrosine kinase 6 directly phosphorylates AKT and promotes AKT activation in response to epidermal growth factor. *Mol Cell Biol*. 2010; 30:4280–4292. [PubMed: 20606012]
39. Castro NE, Lange CA. Breast tumor kinase and extracellular signal-regulated kinase 5 mediate Met receptor signaling to cell migration in breast cancer cells. *Breast Cancer Res*. 2010; 12:R60. [PubMed: 20687930]
40. Brauer PM, Tyner AL. Building a better understanding of the intracellular tyrosine kinase PTK6 – BRK by BRK. *Biochim Biophys Acta*. 2010; 1806:66–73. [PubMed: 20193745]
41. Barrett A, Pellet-Many C, Zachary IC, Evans IM, Frankel P. p130Cas: a key signalling node in health and disease. *Cell Signalling*. 2013; 25:766–777. [PubMed: 23277200]
42. Pellicena P, Miller WT. Processive phosphorylation of p130Cas by Src depends on SH3-polyproline interactions. *J Biol Chem*. 2001; 276:28190–28196. [PubMed: 11389136]

43. Liu L, Gao Y, Qiu H, Miller WT, Poli V, Reich NC. Identification of STAT3 as a specific substrate of breast tumor kinase. *Oncogene*. 2006; 25:4904–4912. [PubMed: 16568091]
44. Locatelli A, Lofgren KA, Daniel AR, Castro NE, Lange CA. Mechanisms of HGF/Met signaling to Brk and Sam68 in breast cancer progression. *Horm Cancer*. 2012; 3:14–25. [PubMed: 22124844]
45. Bielli P, Busa R, Paronetto MP, Sette C. The RNA-binding protein Sam68 is a multifunctional player in human cancer. *Endocr-Relat Cancer*. 2011; 18:R91–R102. [PubMed: 21565971]
46. Lukong KE, Larocque D, Tyner AL, Richard S. Tyrosine phosphorylation of sam68 by breast tumor kinase regulates intranuclear localization and cell cycle progression. *J Biol Chem*. 2005; 280:38639–38647. [PubMed: 16179349]
47. Chen T, Boisvert FM, Bazett-Jones DP, Richard S. A role for the GSG domain in localizing Sam68 to novel nuclear structures in cancer cell lines. *Mol Biol Cell*. 1999; 10:3015–3033. [PubMed: 10473643]
48. Derry JJ, Richard S, Valderrama Carvajal H, Ye X, Vasioukhin V, Cochrane AW, Chen T, Tyner AL. Sik (BRK) phosphorylates Sam68 in the nucleus and negatively regulates its RNA binding ability. *Mol Cell Biol*. 2000; 20:6114–6126. [PubMed: 10913193]
49. Palka-Hamblin HL, Gierut JJ, Bie W, Brauer PM, Zheng Y, Asara JM, Tyner AL. Identification of beta-catenin as a target of the intracellular tyrosine kinase PTK6. *J Cell Sci*. 2010; 123:236–245. [PubMed: 20026641]
50. Futreal PA, Coin L, Marshall M, Down T, Hubbard T, Wooster R, Rahman N, Stratton MR. A census of human cancer genes. *Nat Rev Cancer*. 2004; 4:177–183. [PubMed: 14993899]
51. Pleasance ED, Cheetham RK, Stephens PJ, McBride DJ, Humphray SJ, Greenman CD, Varela I, Lin ML, Ordonez GR, Bignell GR, Ye K, Alipaz J, Bauer MJ, Beare D, Butler A, Carter RJ, Chen L, Cox AJ, Edkins S, Kokko-Gonzales PI, Gormley NA, Grocock RJ, Haudenschild CD, Hims MM, James T, Jia M, Kingsbury Z, Leroy C, Marshall J, Menzies A, Mudie LJ, Ning Z, Royce T, Schulz-Trieglaff OB, Spiridou A, Stebbings LA, Szajkowski L, Teague J, Williamson D, Chin L, Ross MT, Campbell PJ, Bentley DR, Futreal PA, Stratton MR. A comprehensive catalogue of somatic mutations from a human cancer genome. *Nature*. 2010; 463:191–196. [PubMed: 20016485]
52. Blume-Jensen P, Hunter T. Oncogenic kinase signalling. *Nature*. 2001; 411:355–365. [PubMed: 11357143]
53. Ludyga N, Anastasov N, Gonzalez-Vasconcellos I, Ram M, Hofler H, Aubele M. Impact of protein tyrosine kinase 6 (PTK6) on human epidermal growth factor receptor (HER) signalling in breast cancer. *Mol BioSyst*. 2011; 7:1603–1612. [PubMed: 21380407]
54. Regan Anderson TM, Peacock DL, Daniel AR, Hubbard GK, Lofgren KA, Girard BJ, Schorg A, Hoogewijs D, Wenger RH, Seagroves TN, Lange CA. Breast tumor kinase (Brk/PTK6) is a mediator of hypoxia-associated breast cancer progression. *Cancer Res*. 2013; 73:5810–5820. [PubMed: 23928995]
55. Ma S, Bao JY, Kwan PS, Chan YP, Tong CM, Fu L, Zhang N, Tong AH, Qin YR, Tsao SW, Chan KW, Lok S, Guan XY. Identification of PTK6, via RNA sequencing analysis, as a suppressor of esophageal squamous cell carcinoma. *Gastroenterology*. 2012; 143:675–686. e671–612. [PubMed: 22705009]
56. Chen YF, Ma G, Cao X, Huang ZL, Zeng MS, Wen ZS. Downregulated expression of PTK6 is correlated with poor survival in esophageal squamous cell carcinoma. *Med Oncol*. 2014; 31:317. [PubMed: 25377660]
57. Liu XK, Zhang XR, Zhong Q, Li MZ, Liu ZM, Lin ZR, Wu D, Zeng MS. Low expression of PTK6/Brk predicts poor prognosis in patients with laryngeal squamous cell carcinoma. *J Transl Med*. 2013; 11:59. [PubMed: 23497344]
58. Le PN, McDermott JD, Jimeno A. Targeting the Wnt pathway in human cancers: Therapeutic targeting with a focus on OMP-54F28. *Pharmacol Ther*. 2015; 146C:1–11. [PubMed: 25172549]
59. Brauer PM, Zheng Y, Evans MD, Dominguez-Brauer C, Peehl DM, Tyner AL. The alternative splice variant of protein tyrosine kinase 6 negatively regulates growth and enhances PTK6-mediated inhibition of beta-catenin. *PLoS One*. 2011; 6:e14789. [PubMed: 21479203]

60. Ie Kim H, Lee ST. Oncogenic functions of PTK6 are enhanced by its targeting to plasma membrane but abolished by its targeting to nucleus. *J Biochem.* 2009; 146:133–139. [PubMed: 19304789]

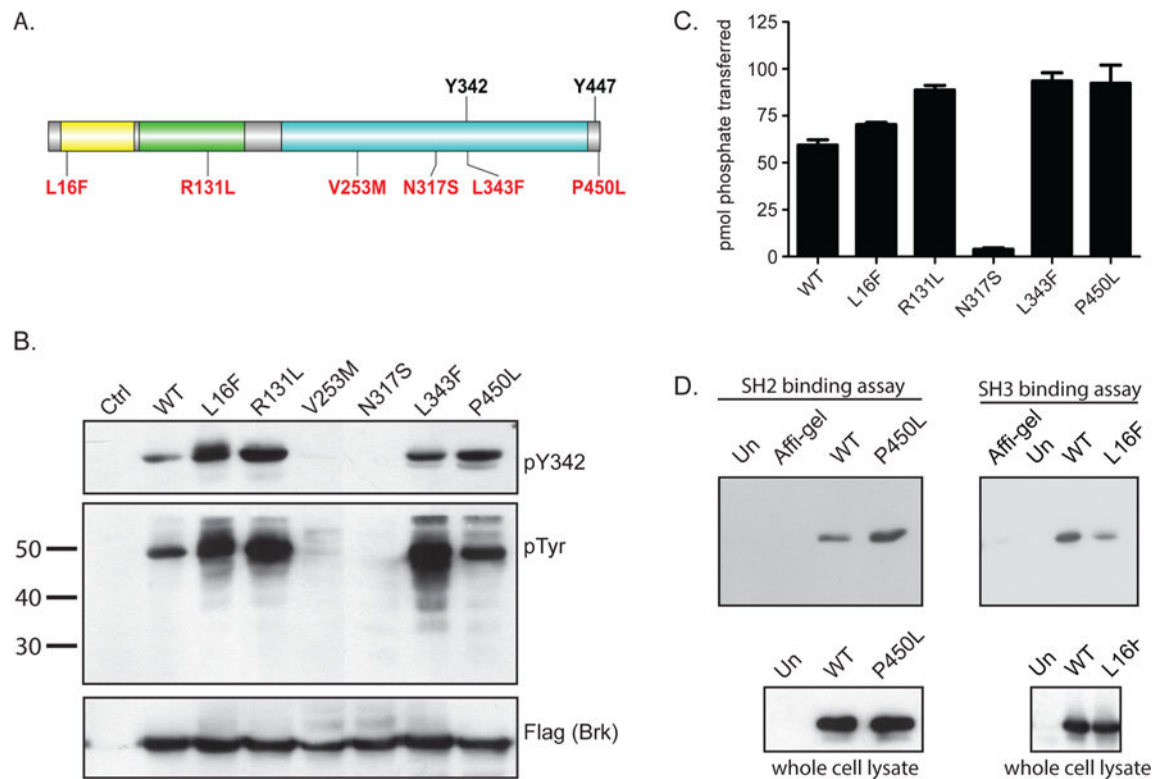
Author Manuscript

Author Manuscript

Author Manuscript

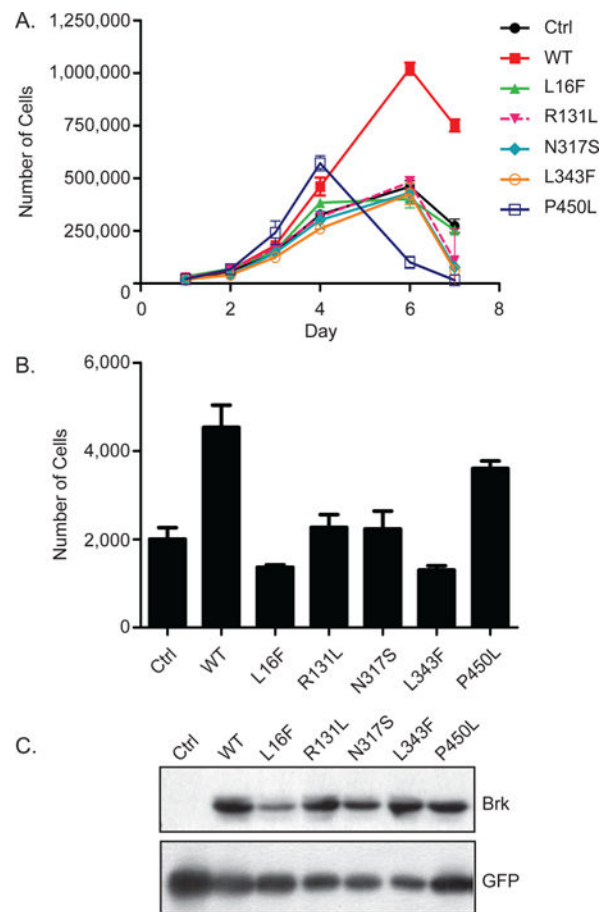
Author Manuscript





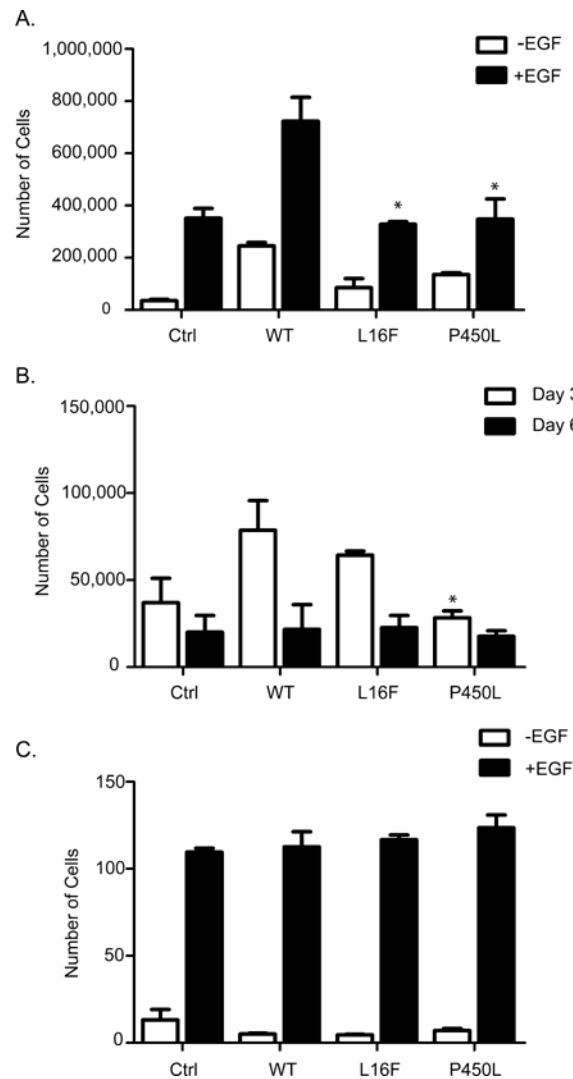
**Figure 1.**

Cancer-associated mutations affect Brk activation and intramolecular interactions. (A) The domain arrangement of Brk is shown schematically. The autophosphorylation site (Tyr 342) and inhibitory tyrosine (Tyr 447) are in black. The cancer-associated mutations are indicated in red. (B) Lysates from 293T cells expressing Flag-tagged wild-type or mutant forms of Brk were probed with anti-phosphoBrk (pY342), phosphotyrosine, and Flag antibodies. The gel is representative of five similar experiments. (C) Wild-type and mutant forms Brk were immunoprecipitated from transfected 293T cells using anti-Flag M2 affinity gel, then incubated with Src-substrate peptide in the presence of [ $\gamma^{32}$ -P] ATP. The activities were measured in duplicate with the phosphocellulose paper assay. The results are representative of three experiments. The error bars show standard deviations. (D) Lysates from Src<sup>-</sup>Yes<sup>-</sup>Fyn<sup>-</sup> null (SYF) cells expressing wild-type or mutant forms of Brk were incubated with SH2 ligand (left) or SH3 ligand (right) conjugated to agarose beads. Bound protein was eluted with SDS-PAGE sample buffer and resolved by SDS-PAGE, then probed with anti-Brk (left) and anti-Flag (right) antibodies. Affi-gel control samples contained lysates from wild-type Brk expressing cells incubated with nonconjugated beads. Untransfected controls (Un) contained untransfected cell lysates with peptide conjugated beads.



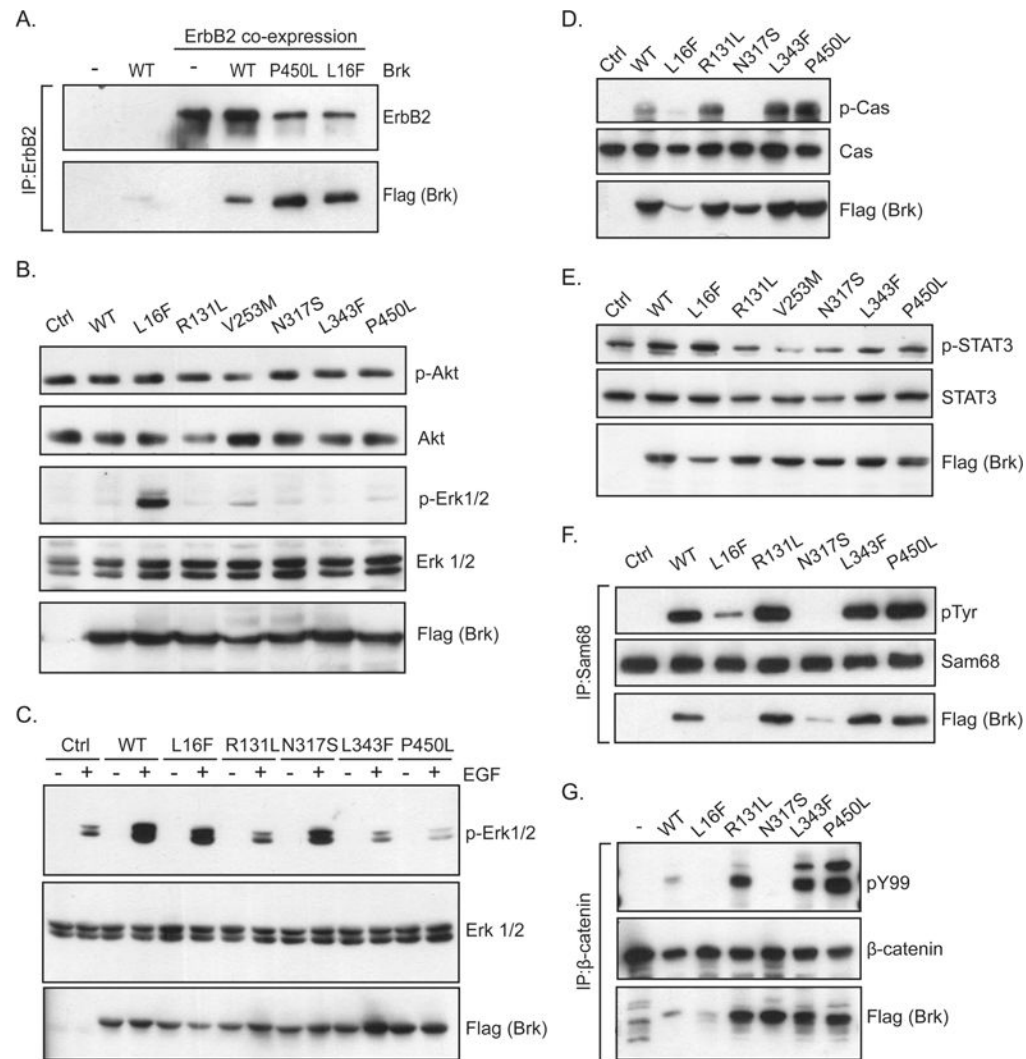
**Figure 2.**

Effect of Brk mutants on cell growth. (A) Anchored cell growth: 20 000 NIH-3T3 cells stably expressing wild-type or mutant Brk were plated in duplicate in 12-well plates and counted over several days with a hemocytometer. The results are representative of three experiments. The error bars represent standard deviations. (B) Nonanchored cell growth: 20 000 NIH-3T3 stable cells were plated in triplicate in 24-well low attachment plates. On day 6, the cells were collected and counted using a hemocytometer. The results are representative of two experiments. The error bars represent standard deviations. (C) Lysates from NIH3T3 cells expressing wild type or mutant forms of Brk were probed with anti-Brk and anti-GFP antibodies.



**Figure 3.**

Biological effects of Brk mutants in MCF-10a cells. (A) MCF-10a cells (20 000) stably expressing wild-type or mutant forms of Brk were plated in 24-well plates in starvation media. Eighteen hours post-starvation, cells were stimulated with 2.5 ng/mL EGF or were left untreated. Cells were counted on a hemocytometer 6 days after EGF stimulation. The data is representative of three similar experiments. The error bars show standard deviations. \* $P < 0.05$  compared to Brk WT. (B) MCF-10a cells (50 000) were plated in a 24-well low attachment plate. On days 3 and 6, the cells were collected and counted using a hemocytometer. The data is representative of three similar experiments. The error bars show standard deviations. \* $P < 0.05$  compared to Brk WT. (C) MCF-10a cells (100 000) were serum starved for 24 h then were plated in Transwell inserts of a 24-well plate. Media with or without 15 ng/mL EGF was added to the bottom chamber. After 8 h, migrated cells were fixed then stained with DAPI, and imaged with a fluorescent microscope and counted with ImageJ software. The number of cells is the average of cells counted in 5 fields per well. The error bars show standard deviations.

**Figure 4.**

Effect of Brk mutants on signaling pathways. (A) 293T cells coexpressing ErbB2 and wild-type or mutant forms of Brk were incubated with anti-ErbB2 antibody. Immunoprecipitated protein was eluted with SDS-PAGE sample buffer and probed with anti-ErbB2 and anti-Flag antibodies. (B) 293T cells expressing wild-type or mutant forms of Brk were probed with anti-phospho-Akt (Ser473), anti-Akt, anti-phospho-Erk1/2 (Thr202/Tyr204), anti-Erk1/2, and anti-Flag antibodies. (C) 293T cells were stimulated with 10 ng/mL EGF for 2.5 min following overnight serum starvation. Lysates were probed with anti-phospho-Erk1/2 (Thr202/Tyr204), anti-Erk1/2, and anti-Flag antibodies. (D) Lysates from 293T cells expressing both p130Cas and wild-type or mutant forms of Brk were probed with anti-phospho-p130Cas (Tyr 249), anti-p130Cas, and anti-Flag antibodies. (E) 293T cells expressing wild-type or mutant forms of Brk were probed with anti-phospho-STAT3 (Tyr 507), anti-STAT3, and anti-Flag antibodies. (F) Endogenous Sam68 protein was immunoprecipitated from 293T cells expressing wild-type or mutant forms of Brk using anti-Sam68 antibody. Immunoprecipitated proteins were eluted with SDS-PAGE sample buffer and probed with anti-phosphotyrosine, anti-Sam68, and anti-Flag antibodies. (G)  $\beta$

Catenin was immunoprecipitated from 293T cells expressing  $\beta$ -catenin and wild-type or mutant forms of Brk. Immunoprecipitated proteins were eluted with SDS-PAGE sample buffer and probed with an anti-phosphotyrosine, anti- $\beta$ -catenin, and anti-Flag antibodies.

Author Manuscript

Author Manuscript

Author Manuscript

Author Manuscript

**Table 1**

Summary of Mutant Effects on Brk Autophosphorylation and Substrate Activation<sup>a</sup>

	ctrl	WT	L16F	R131L	N317S	L343F	P450L
autophosphorylation	-	+	+++	+++	-	+++	++
ErbB2 interaction	-	+	+++	ND	ND	ND	+++
p-Akt	+	+	+	+	+	+	+
p-Erk1/2	+	+	+++	+	+	+	+
p-Erk1/2 + EGF	-	+	+	-	+	-	-
p-Cas	-	+	-	++	-	+++	+++
p-STAT3	-	+	+	-	-	+	+
p-Sam68	-	+	-	++	-	++	++
p- $\beta$ -Catenin	-	+	-	++	-	+++	+++

<sup>a</sup> A minus sign (-) indicates a signal that was less than that of WT. A plus sign (+) indicates a signal that was similar to that of the WT, and increasing numbers of plus signs indicate signals stronger than that of the WT. ND, not determined.